

Large Language Models Are Human-Like Internally

Tatsuki Kuribayashi¹ Yohei Oseki² Souhaib Ben Taieb^{1,3}
Kentaro Inui^{1,4,5} Timothy Baldwin^{1,6}

¹MBZUAI ²The University of Tokyo ³University of Mons
⁴Tohoku University ⁵RIKEN ⁶The University of Melbourne
{tatsuki.kuribayashi, souhaib.bentaieb,
kentaro.inui, timothy.baldwin}@mbzuai.ac.ae
oseki@g.ecc.u-tokyo.ac.jp

Abstract

Recent cognitive modeling studies have reported that larger language models (LMs) exhibit a poorer fit to human reading behavior (Oh and Schuler, 2023b; Shain et al., 2024; Kuribayashi et al., 2024), leading to claims of their cognitive implausibility. In this paper, we revisit this argument through the lens of mechanistic interpretability and argue that prior conclusions were skewed by an exclusive focus on the final layers of LMs. Our analysis reveals that next-word probabilities derived from internal layers of larger LMs align with human sentence processing data as well as, or better than, those from smaller LMs. This alignment holds consistently across behavioral (self-paced reading times, gaze durations, MAZE task processing times) and neurophysiological (N400 brain potentials) measures, challenging earlier mixed results and suggesting that the cognitive plausibility of larger LMs has been underestimated. Furthermore, we first identify an intriguing relationship between LM layers and human measures: earlier layers correspond more closely with fast gaze durations, while later layers better align with relatively slower signals such as N400 potentials and MAZE processing times. Our work opens new avenues for interdisciplinary research at the intersection of mechanistic interpretability and cognitive modeling.

1 Introduction

Understanding human sentence processing has long been a fundamental goal in linguistics. This goal is typically approached by investigating *what computational models can simulate human sentence processing data*, such as eye movement patterns during reading, in the field of computational psycholinguistics (Crocker, 2007; Beinborn and

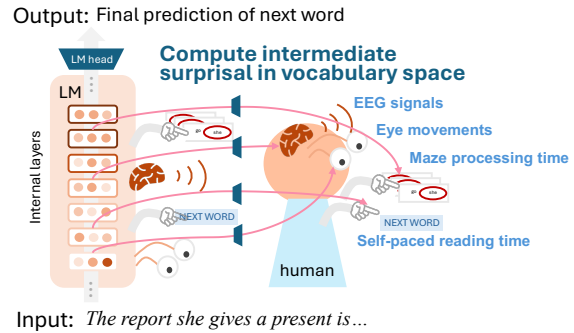


Figure 1: Different measures of human sentence processing align with surprisal from different layers of language models (LMs), and the best layer is typically not the final one. Larger LMs can better simulate human reading data with their internal layer than smaller LMs.

Hollenstein, 2024). Natural language processing (NLP) models, such as neural language models (LMs), have played a crucial role in this endeavor, serving as tools to test linguistic hypotheses. Specifically, the theory of expectation-based human sentence processing (Hale, 2001; Levy, 2008; Smith and Levy, 2013) — which posits that humans continuously predict upcoming linguistic information during reading — naturally raises the following questions: how well do word probabilities (i.e., surprisal, $-\log p(\text{word}|\text{context})$) derived from LMs align with human sentence processing behavior? What kind of LMs produce the most human-like surprisal?

Previous studies have provided substantial evidence supporting expectation-based accounts of human sentence processing (Shain et al. 2024; *inter alia*). However, they reveal an intriguing trend: surprisal estimates from large language models (LLMs) often deviate from human reading behavior, and rather smaller models, such as GPT-2 small, offer better simulations of human behavior (Shain et al., 2024; Oh and Schuler, 2023b;

Kuribayashi et al., 2022, 2024). This observation — *larger LMs are less human-like* — has sparked intriguing linguistic questions (Wilcox et al., 2024) as well as a fair amount of confusion within the community. Why do smaller LMs appear more human-like, despite their generally poorer linguistic competence (Waldis et al., 2024)?

In this work, we highlight the cognitively *plausible* aspects of LLMs, challenging existing conclusions. Specifically, we show that **surprisal derived from the internal layers of larger LMs aligns with human sentence processing data as well as, or even better than, that from smaller LMs**. Previous studies, focusing exclusively on final-layers’ surprisal, have overlooked this critical insight. These results could be drawn with techniques from mechanistic interpretability (Dar et al., 2023; Belrose et al., 2023; Wendler et al., 2024), *logit lens* (nostalgebraist, 2020) or dubbed *early exits* (Kaya et al., 2019); we compute next-word surprisals directly from internal layers of LMs by projecting intermediate representations into the output vocabulary space, bypassing subsequent layers. We additionally revealed that surprisal from earlier layers fits better with fast human responses (first-pass gaze durations and self-paced reading time), while surprisal from later layers aligns more closely with slower measures (N400 and MAZE task data) (Figure 1). This also resolves the previously suggested *behavior–neurophysiology gap* in LM-based cognitive modeling: smaller LMs predict reading behavior better (Oh and Schuler, 2023b), while larger LMs excel in modeling neurophysiological data (Schrimpf et al., 2021; Michaelov et al., 2024a; Hosseini et al., 2024). We would suggest that this gap stemmed from the inconsistent treatment of internal layers (e.g., exclusive reliance on final layers, or inconsistent inclusion of intermediate layers). If all the internal layers were focused on, even larger LMs have human-like layers through the lens of both behavioral and neurophysiological data.

Our exploration aligns with the common view that different human measures, operating on distinct timescales, reflect somewhat different stages of sentence processing. For example, fast responses, such as first-pass gaze durations (~200ms), capture early-stage lexical processing (Calvo and Meseguer, 2002), while slower responses, such as N400 event-related potentials

(~400ms), correspond to deeper semantic integration (Lau et al., 2008; Kutas and Federmeier, 2011; Nour Eddine et al., 2024). Analogously, internal layers of LLMs may encode these temporal distinctions: earlier layers align with fast, shallow processes, while later layers correspond to slower, richer processes (Tenney et al., 2019).

In summary, our results suggest that larger LMs provide superior cognitive plausibility in modeling both human behavior and neurophysiology data internally. In other words, shallower, cognitively plausible LMs are “nested” within LLMs. Broadly, these findings advocate the integration of cognitive modeling and mechanistic interpretability, encouraging a focus on layer-wise alignment with human measures.

2 Related Work

2.1 Cognitive modeling and NLP

A key objective in linguistics is to understand how humans process language (Crocker, 2007), a goal that remains pertinent even in the era of LLMs. According to perspectives outlined by Marr (1982), information processing can be examined at three levels: (i) the computational level—*what is the goal of computation?*, (ii) the algorithmic level—*how does the model achieve the goal?*, and (iii) the implementational level—*how is it physically implemented?*. Humans can be viewed as an information processing model, and surprisal theory (Hale, 2001; Levy, 2008; Smith and Levy, 2013) provides empirical evidence as a computational-level explanation of human sentence processing (Smith and Levy 2013; Frank et al. 2015; Shain et al. 2024; *inter alia*).¹ According to surprisal theory, humans continuously predict upcoming information during reading, with cognitive load incurred by unpredictable information.

Once the computational-level theory is assumed, the next question can be more relevant to the algorithmic level: *with what kind of algorithms and representations, humans predict upcoming information*. The NLP community has developed various methods to compute next-word probabilities, ranging from N-gram models to

¹Surprisal theory has also been critiqued (van Schijndel and Linzen, 2021; Huang et al., 2024), particularly for its failure to account for the cognitive load incurred in complex sentences. Our contribution will be orthogonal to such criticism (see Limitation section).

LLMs. By exploring which NLP models best simulate human sentence processing, researchers can bridge the models demanded in psycholinguistics (language processing in humans) and those implemented in NLP (language processing in machines). This alignment is typically investigated by analyzing which LMs compute surprisal $-\log p(\text{word}|\text{context})$ that correlates with human measures (e.g., word-by-word gaze durations) based on the surprisal theory. Orthogonal to the exploration of various model architectures, this study investigates in which part/layer of a model human-like measures emerge.

2.2 Poorer fit of larger LMs’ surprisal to human reading behavior

Before the advent of LLMs, models such as incremental parsers (Levy, 2008), N-gram LMs (Smith and Levy, 2013), RNN-based LMs (Frank and Bod, 2011; Aurnhammer and Frank, 2019), Transformer-based LMs (Merx and Frank, 2021), and syntactic LMs (Hale et al., 2018; Yoshida et al., 2021; Oh et al., 2021, 2022) were extensively analyzed in cognitive modeling. In the days of much smaller LMs than modern LLMs, LM-scaling generally improved their ability to simulate human sentence processing data (Frank and Bod, 2011; Goodkind and Bicknell, 2018; Wilcox et al., 2020, 2023a). However, recent studies have questioned the generality of this scaling effect. The reversed trend was first found in typologically distant languages (Kuribayashi et al., 2021), and even within English, further scaling up LMs have shown weaker alignment with human reading behavior (Kuribayashi et al., 2022; Shain et al., 2024; Oh and Schuler, 2023b). This *bigger is not always better* phenomenon has become a key focus of LM-based cognitive modeling (Wilcox et al., 2024), with researchers investigating why LLMs appear cognitively implausible (Kuribayashi et al., 2022; Oh and Schuler, 2023a,b; Oh et al., 2024; Nair and Resnik, 2023; Kuribayashi et al., 2024). This study contributes to this discussion from a different perspective: We show the cognitively plausible properties of LLMs rather than solely identifying their limitations.

In addition, recent studies have typically reported *behavior–neurophysiology gap* in LM-scaling effects (Michaelov et al., 2024a; Aw et al., 2024); smaller LMs simulate reading behavior better (Oh and Schuler, 2023b), while larger LMs

simulate neurophysiological data better (Schrimpf et al., 2021; Michaelov et al., 2024a; Hosseini et al., 2024). Opposite effect of instruction-tuning was also observed between brain data and behavioral data (Aw et al., 2024; Kuribayashi et al., 2024). We begin by offering a perspective to address this gap, showing that the internal layers of larger LMs are more effective at modeling both behavioral and neurophysiological data.

2.3 Mapping different human measures with different LM layers

We analyze the next-word predictions from the internal layers of LLMs in comparison with human sentence processing data. One motivation for this analysis is that different human measures, particularly at different time scales, may emphasize different stages of sentence processing (Witzel et al., 2012; Lewis and Vasishth, 2005; Vani et al., 2021; Caucheteux et al., 2023; McCurdy and Hahn, 2024). LM internal layers, which are also computed sequentially, would be a natural counterpart to such multiple stages of processing (Tenney et al., 2019). For example, eye movements reach the next word (or further) typically in $\sim 200\text{ms}$ before N400 brain signals peak at $\sim 400\text{ms}$ (Dimigen et al., 2011), suggesting that fast gaze durations may not reflect the cognitive load indexed by N400 signals (Rayner and Clifton, 2009).

Furthermore, self-paced reading and eye-tracking measures often exhibit *spillover effects*, where the processing of one word influences subsequent words (Rayner, 1998). This suggests that the comprehension of a word extends beyond the immediate moment, and the associated reading times may only capture an early stage of processing. In contrast, the MAZE task (Forster et al., 2009; Boyce and Levy, 2023), which measures the time taken to select a plausible continuation from two candidates, mitigates spillover effects and is thus expected to reflect the full process of word processing. Our findings align with this perspective. Early LM layers are more closely aligned with gaze durations and self-paced reading times, while later layers show a stronger alignment with MAZE, as discussed in § 4.

Note that similar layer-wise LM-brain alignments have been attempted in fMRI modeling research (Toneva and Wehbe, 2019; Schrimpf et al., 2021; Caucheteux et al., 2023) and suggested that different brain areas better align with different LM

layers. They typically trained linear regression models to predict brain activity directly using d -dimensional LM internal representations $\mathbf{h} \in \mathbb{R}^d$ as features, instead of using surprisal measures $-\log p(\text{word}|\text{context}) \in \mathbb{R}_{\geq 0}$. Thus, their results are not comparable with existing surprisal-based studies and may rather suffer from a confounding factor of different d for different LMs when precisely discussing LM-scaling effects.

2.4 Early exits of neural models’ prediction

In the engineering context, predictions from internal layers of deep neural networks (i.e., early exits of the results from internal layers) are used to improve inference efficiency by avoiding their overthinking (Graves, 2016; Banino et al., 2021), which is also called adaptive computation time (Kaya et al., 2019; Zhou et al., 2020). Such technique has also recently been employed to enhance interpretability research to identify at which layer a particular prediction shapes (nostalgebraist, 2020; Dar et al., 2023; Belrose et al., 2023). We apply *logit lens* (nostalgebraist, 2020) and its variant of *tuned lens* (Belrose et al., 2023), projecting intermediate representations to the output space, to extract next-word predictions from the internal layers of LLMs.

3 Experimental Settings

3.1 Human Data

Table 1 lists the 15 human reading datasets used in our study (we additionally use MECO in § 5.4), which include human measurements from various methods: self-paced reading time (SPR), first-pass gaze duration (FPGD), Maze task processing time (MAZE), and electroencephalography (EEG; specifically the N400 component). The datasets share a common format: each word w_t is annotated with $\text{Cost}(w_t) \in \mathbb{R}$ representing the human cognitive load associated with it. Our corpus selection aligns with recent studies (Kuribayashi et al., 2024; Michaelov et al., 2024a; de Varda et al., 2024; McCurdy and Hahn, 2024).²

SPR is measured by presenting sentences through a sliding word-by-word window, with participants pressing a button to advance. FPGD, a

²We applied the same preprocessing as Kuribayashi et al. (2024) (DC, NS), de Varda et al. (2024) (UCL), Hahn et al. (2022) (Fillers), and Michaelov et al. (2024a) (N400). For ZuCO, we only used the naturalistic reading part, and for its N400, we averaged the values at the central electrode between 300-500ms during the first pass over a word.

key eye-tracking measure, represents the total time from first fixating on a word to moving to another word. Maze processing time is measured during a task requiring participants to select the plausible continuation of a sentence, offering a controlled alternative to naturalistic reading. EEG measures brain activity, with N400 reflecting the negative brain potential peaking around 400ms after word presentation. These are the common measures employed to study expectation-based sentence processing. SPR, FPGD, and MAZE are categorized as human *behavioral* data, while EEG falls under *neurophysiological* data.

To minimize confounding factors between stimuli data and human measures, we included datasets with multi-layered annotations across multiple human measures. These include the Natural Stories Corpus (Futrell et al., 2021) with SPR and MAZE data (Boyce and Levy, 2023), ZuCO corpus (Hollenstein et al., 2018) with FPGD and N400 data, UCL Corpus (Frank et al., 2013) annotated with SPR, FPGD, and N400 data (Frank et al., 2015), and filler sentences from Hahn et al. (2022) annotated with SPR, FPGD, and MAZE data (Vasishth et al., 2010; Hahn et al., 2022). In particular, the FPGD and N400 data in ZuCO were simultaneously recorded from the same human subjects, which likely minimized confounding factors.

3.2 Language Models

We evaluated 21 open-source LMs including billion-scale ones: GPT-2 (124M, 355M, 774M, and 1.5B parameters) (Radford et al., 2019), OPT (125M, 1.3B, 2.7B, 6.7B, 13B, 30B, and 66B parameters) (Zhang et al., 2022), and Pythia (14M, 31M, 70M, 160M, 410M, 1B, 1.4B, 2.8B, 6.9B, and 12B parameters) (Biderman et al., 2023). For tuned-lens experiments (§ 3.4), we used 14 of these models based on the availability of pre-trained tuned lenses.³ The number of internal layers in our models ranges from 6 to 64. Results for surprisal from the embedding layer are excluded.

3.3 Psychometric Predictive Power

We evaluated the ability of surprisal values $\text{surprisal}(w_t) \in \mathbb{R}_{\geq 0}$ to predict word-by-word human reading data $\text{Cost}(w_t) \in \mathbb{R}$ using regression models with several baseline features:

³GPT-2 124M, 774M, 1.5B; OPT 125M, 1.3B, 6.7B; and Pythia 70M, 160M, 410M, 1B, 1.4B, 2.8B, 6.9B, 12B.

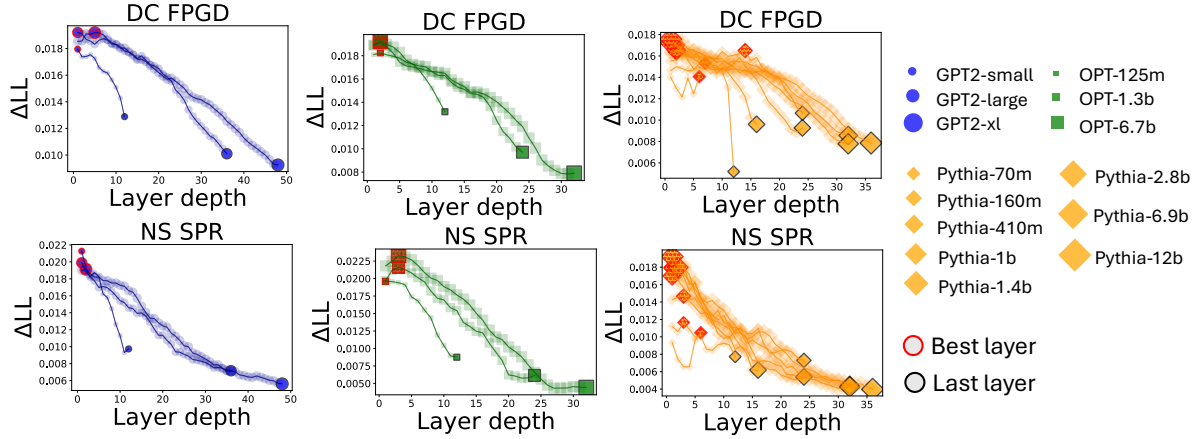


Figure 2: Relationships between layer depth (x-axis) and ΔLL (y-axis) for each LM in two datasets: FPGD in DC and SPR in NS. The graphs are separated by model families and data. The best/last layer is indicated with a red/black edge line. The graph starts at the first layer, not at the embedding layer.

$$\begin{aligned}
 \text{Cost}(w_t) &\sim \text{surprisal}(w_t) + \text{surprisal}(w_{t-1}) \\
 &\quad + \text{surprisal}(w_{t-2}) \\
 &\quad + \text{length}(w_t) + \text{freq}(w_t) \\
 &\quad + \text{length}(w_{t-1}) + \text{freq}(w_{t-1}) \\
 &\quad + \text{length}(w_{t-2}) + \text{freq}(w_{t-2}) . \quad (1) \\
 \text{surprisal}(w_t) &= -\log p(w_t | \mathbf{w}_{<t}) . \quad (2)
 \end{aligned}$$

Here, w_t is t -th word in a text, and $\mathbf{w}_{<t} = [w_1, \dots, w_{t-1}]$ is its context. Length and unigram frequency of words are included as baseline factors,⁴ and $\text{surprisal}(w_{t-1}) \in \mathbb{R}_{\geq 0}$ and $\text{surprisal}(w_{t-2}) \in \mathbb{R}_{\geq 0}$ are also added to account for spillover effects. This model design follows recent studies (Wilcox et al., 2023b; Pimentel et al., 2023),⁵. We used statsmodels package (Seabold and Perktold, 2010).

We trained linear regression models both with and without $\text{surprisal}(w_t)$, and we report the difference in the goodness of fit measured by log-likelihood (Δ log-likelihood; ΔLL). This indicates how strongly surprisal contributes to predicting human sentence processing data, i.e., higher ΔLL is better. The key question is which LM layer computes surprisal with better ΔLL .

Note that we used the same baseline factors across all datasets/models for a fair comparison, except for electrode random effects for Michaelov et al. (2024b)’s EEG data. As is common in preprocessing, we exclude data points with zero SPR/FPGD/MAZE. Human data for each token in the corpus were averaged across subjects prior

⁴Word length follows character number, and word frequency is estimated with `word_freq` (Speer, 2022).

⁵For N400 data, we added baseline amplitude feature.

to analysis, following recent practices (Pimentel et al., 2023; Oh and Schuler, 2023b; Kuribayashi et al., 2024; de Varda et al., 2024).

3.4 Probabilities from internal layers

Let us begin with the simplest method of *logit-lens* (nostalgebraist, 2020) to extract the probability of a word w_t from model internals. Given a d -dimensional internal representation $\mathbf{h}_{l,t} \in \mathbb{R}^d$ at the l -th layer and time step t , the probability of a word w_t in its context $\mathbf{w}_{<t}$ is obtained as follows:

$$\begin{aligned}
 p(w_t | \mathbf{w}_{<t}; \mathbf{h}_{l,t}) &= \text{LogitLens}(\mathbf{h}_{l,t})[\text{id}(w_t)] \\
 &= \text{softmax}(\text{LayerNorm}(\mathbf{h}_{l,t}) \mathbf{W}_U) [\text{id}(w_t)], \quad (3)
 \end{aligned}$$

where $\mathbf{W}_U \in \mathbb{R}^{d \times |\mathcal{V}|}$ is an unembedding matrix obtained from LM’s output layer, and $|\mathcal{V}| \in \mathbb{R}$ is model’s vocabulary size. Simply put, the internal representation $\mathbf{h}_{l,t}$ is mapped into output vocabulary space by applying \mathbf{W}_U (i.e., skipping subsequent layers $[\mathbf{h}_{l+1,t}, \dots, \mathbf{h}_{\text{last},t}]$), and next-word probability is obtained in that space. The obtained probability (Eq. 3) is first transformed to surprisal (Eq. 2), and then used in the regression model to predict human reading data (Eq. 1). $\text{LayerNorm}(\cdot)$ in Eq. 3 is the layer normalization at the last layer, and $[\text{id}(w_t)]$ extracts the probability for w_t ⁶ from the probability distribution over \mathcal{V} , obtained through the $\text{softmax}(\cdot) : \mathbb{R}^{|\mathcal{V}|} \rightarrow [0, 1]^{|\mathcal{V}|}$ function.

Building on the logit-lens, Belrose et al. (2023) extended the method into *tuned-lens* to handle

⁶If a word is split into multiple subwords, accumulated surprisal is used. See Eq.2 in Kuribayashi et al. (2021).

Stimuli	Measure	Logit-lens (Δ LL)					Tuned-lens (Δ LL)				
		0-0.2	0.2-0.4	0.4-0.6	0.6-0.8	0.8-1.0	0-0.2	0.2-0.4	0.4-0.6	0.6-0.8	0.8-1.0
DC (Dundee corpus)	FPGD (Kennedy et al., 2003)	16.49	17.75	17.41	15.13	10.44	17.10	16.32	15.39	13.53	10.49
NS (Natural Stories Corpus)	SPR (Futrell et al., 2021)	23.59	23.75	21.16	13.37	7.11	16.88	14.53	11.36	8.14	6.32
	MAZE (Boyce and Levy, 2023)	1.63	4.26	8.22	18.19	31.81	9.70	17.56	24.15	32.86	39.63
ZuCO	FPGD (Hollenstein et al., 2018)	34.84	35.39	31.97	23.08	9.75	30.48	27.16	22.56	17.29	8.77
	N400 (Hollenstein et al., 2018)	0.06	0.10	0.15	0.20	0.15	0.20	0.32	0.34	0.29	0.18
UCL	SPR (Frank et al., 2013)	24.51	23.35	18.84	7.80	1.81	15.78	8.92	4.87	2.53	1.27
	FPGD (Frank et al., 2013)	22.62	26.24	25.12	15.55	5.02	16.28	14.48	11.87	9.47	5.57
	N400 (Frank et al., 2015)	57.45	33.30	14.01	12.89	32.26	11.31	6.12	16.19	29.49	37.11
Fillers in Vasishth et al. (2010)	SPR (Vasishth et al., 2010)	7.37	12.11	15.31	15.82	15.75	8.60	10.47	11.36	11.86	13.33
	FPGD (Vasishth et al., 2010)	8.93	8.07	8.44	8.98	12.01	8.94	10.91	12.91	13.81	14.00
	MAZE (Hahn et al., 2022)	4.72	2.99	7.53	35.86	83.16	9.96	28.27	52.00	73.38	88.64
Michaelov+, 2024	N400 (Michaelov et al., 2024b)	1.07	1.79	2.37	2.10	1.13	0.95	1.51	1.70	1.38	0.99
Federmeier+, 2007	N400 (Federmeier et al., 2007)	0.85	3.31	9.87	23.22	27.72	1.49	5.22	13.06	24.48	28.71
W&F, 2012	N400 (Wlotko and Federmeier, 2012)	0.44	0.24	0.09	0.08	0.13	0.51	0.27	0.12	0.05	0.11
Hubbard+, 2019	N400 (Hubbard et al., 2019)	0.18	0.19	0.24	0.30	0.22	0.11	0.12	0.22	0.36	0.33
S&F,2022	N400 (Szewczyk and Federmeier, 2022)	0.13	0.18	0.39	1.02	1.36	0.16	0.33	0.77	1.29	1.42
Szewczyk+, 2022	N400 (Szewczyk et al., 2022)	1.61	3.32	5.07	7.96	8.40	2.12	3.58	5.52	8.10	8.93

Table 1: All the results. The Δ LL scores are averaged by the layer relative depth, e.g., first 20% of layers as “0-0.2,” across models, and the best relative layer range for each data is highlighted in bold. Δ LLs are multiplied by 1000 for brevity.

the potential *representational drifts* through layers. This technique introduces an additional linear transformation for each layer l to mitigate the mismatch between the representation spaces of the l -th layer and the last layer:

$$p(w|\mathbf{w}_{<t}; \mathbf{h}_{l,t}) = \text{LogitLens}(\mathbf{h}_{l,t}\mathbf{W}_l + \mathbf{b}_l)[\text{id}(w)], \quad (4)$$

where $\mathbf{W}_l \in \mathbb{R}^{d \times d}$ and $\mathbf{b}_l \in \mathbb{R}^d$ are additionally trained to align the output of logit-lens with the last layer’s next-word probability distribution on additional LM pretraining data.⁷ Notably, we do not fine-tune any part of the LMs for human data; instead, we observe the emerging correlations between next-word probabilities and human reading measures.

4 Experimental results

Figures 2 (§ 4.1) and 3 (§ 4.2) summarize our main findings, with comprehensive results in Table 1.

4.1 Last layer does not yield the best Δ LL

We first revisit the experimental settings (DC and NS datasets) of Oh and Schuler (2023b). The line

⁷We used publicly available tuned-lens: <https://huggingface.co/spaces/AlignmentResearch/tuned-lens/tree/main>. Their actual implementation used the representation of $\mathbf{h}_{l,t}\mathbf{W}'_l + \mathbf{h}_{l,t} + \mathbf{b}_l = \mathbf{h}_{l,t}(\mathbf{W}'_l + \mathbf{1})\mathbf{b}_l$, but we omit the identity matrix $\mathbf{1} \in \mathbb{R}^{d \times d}$ in Eq. 4 by overriding $\mathbf{W}_l = \mathbf{W}'_l + \mathbf{1}$.

graphs in Figure 2 depict the layer-wise Δ LL for each LM. A consistent pattern emerges in the reading behavior (FPGD/SPR) modeling: the Δ LL decreases toward the final layer (the rightmost, less-transparent, large markers), indicating that the last layer often yields the lowest score compared to the internal layers of the same model. These results challenge the assumption, widely adopted in existing studies, that the last layer is the most reliable indicator of an LM’s cognitive plausibility.

Table 1 presents a detailed breakdown of all the datasets, averaging Δ LL scores across relative layer positions (e.g., 0–0.2 for the first 20% of layers). As shown in Figure 2, the best-performing layer is often not the final one (0.8–1.0). The optimal layer varies based on the type of measurement and stimuli. For instance, SPR and FPGD data are best modeled by earlier layers, whereas MAZE processing times and N400 signals are better captured by later layers (as motivated in § 2.3). Furthermore, the optimal layer for the UCL dataset is among the earlier layers, while for the Fillers dataset, it lies among the later layers (perhaps associated with the complexity of stimuli sentences). The layer–measure interaction are further analyzed in § 5.2. Notably, logit-lens and tuned-lens yielded generally consistent patterns.

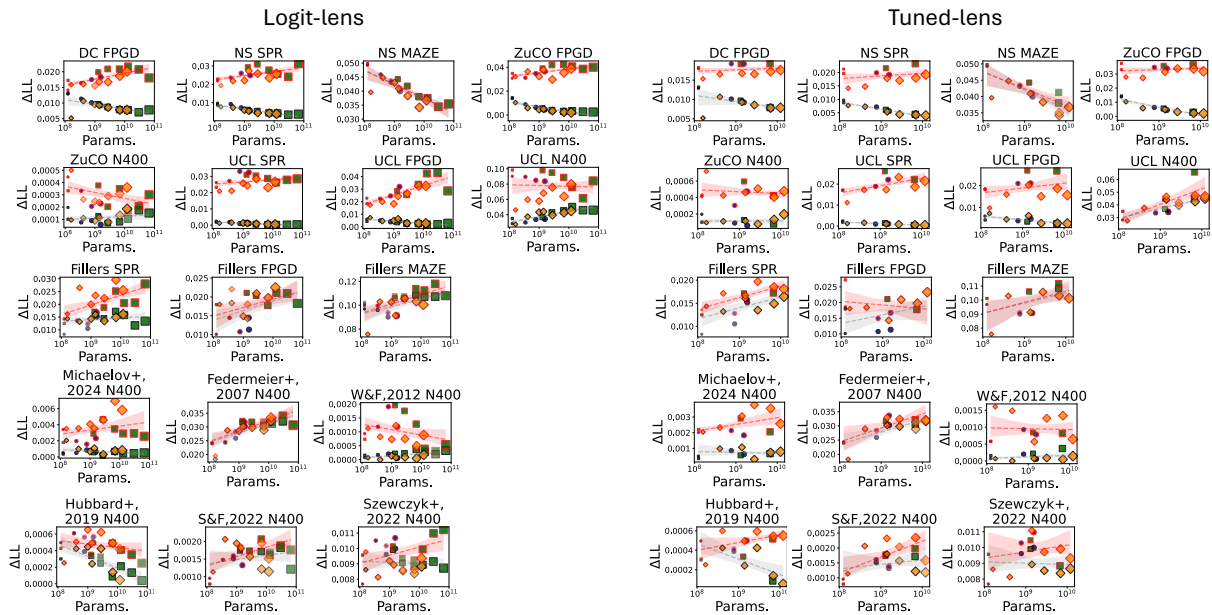


Figure 3: Scaling effect between model size (parameter counts in log scale) and ΔLL . Each marker corresponds to each LM’s ΔLL score from its best layer (red edge) or the last layer (black edge). The regression lines show the scaling effects, and the red line is for best-layer’s ΔLL while the grey one is for the last layer’s. The marker type (shape/size/color) follows the legend in Figure 1. Pythia 14M, 31M, and 70M models are excluded as outliers in the X-axis, but including them does not alter the conclusion.

4.2 Revisiting LM-scaling effects in cognitive modeling with internal layers

We revisit the question with our extended focus on model internals: what kind of LMs yield the best ΔLL from their internals? As the field is particularly interested in the relationship with model scaling (Goodkind and Bicknell, 2018; Oh and Schuler, 2023b), we examine the relationship between LM parameter size (x-axis) and ΔLL (y-axis) for two scenarios: (1) using the last layer’s ΔLL (grey lines), reproducing previous findings, and (2) considering the best ΔLL layer identified in this study (red lines).

Figure 3 illustrates these two relationships. The grey lines align with prior findings replying on the last layer (Oh and Schuler, 2023b; Michaelov et al., 2024a), showing mixed scaling effects, where larger LMs do not consistently outperform smaller ones. However, the red lines reveal a positive scaling trend: larger LMs achieve equal or better ΔLL compared to smaller LMs when internal layers are taken into account. The Pearson correlation coefficients between parameter numbers and ΔLL from the best layers was significantly larger than zero on average, across settings.⁸ This suggests that when the analysis extends to internal

⁸We collected the correlation coefficients between

layers, the ΔLL ranking flips, revealing that larger LMs are seemingly more cognitively plausible. In other words, larger LMs embed cognitively plausible, smaller LMs within their internal. One notable exception is the MAZE processing time in the NS dataset (Boyce and Levy, 2023), where a strictly negative scaling effect persists, even when internal layers are considered. PPL– ΔLL relationships⁹ are additionally shown in Figure 6 in the Appendix, which also show that the poor ΔLL of larger, more accurate LMs is mitigated.

5 Analyses

5.1 How easily can good layers be found?

To assess how many layers yield a good ΔLL , we analyze the amount of internal layers that outperform the previously best ΔLL achieved by the last layer within the same model family. Table 2 presents the win rate of internal layers’ ΔLL against the respective previous best score. The

params. and ΔLL from 34 settings of {dataset} \times {lens}, and one-sample t-test shows that these coefficients are, on average, significantly larger than zero (p-value < 0.05).

⁹Perplexity (PPL), a general quality measure of LMs, is a geometric mean of next-word probabilities over data L : $\prod_{t=1}^L p(w_t | w_{<t})^{1/L}$. The PPL– ΔLL relationship has long been investigated (Frank and Bod, 2011; Goodkind and Bicknell, 2018; Kuribayashi et al., 2021; Oh and Schuler, 2023b).

Data	Logit-lens (win rate)												Tuned-lens (win rate)								
	GPT2 XL	OPT 1.3B	OPT 2.7B	OPT 6.7B	OPT 13B	OPT 30B	OPT 66B	PT 1B	PT 1.4B	PT 2.8B	PT 6.9B	PT 12B	GPT2 XL	OPT 1.3B	OPT 2.7B	OPT 6.7B	PT 1.4B	PT 2.8B	PT 6.9B	PT 12B	
DC FPGD (Kennedy et al., 2003)	0.80	0.80	0.82	0.76	0.73	0.76	0.78	0.00	0.32	0.36	0.73	0.73	0.73	0.80	0.67	0.64	0.58	0.55	0.54		
NS SPR (Futrell et al., 2021)	0.82	0.80	0.85	0.76	0.73	0.76	0.85	0.47	0.52	0.45	0.21	0.41	0.55	0.76	0.70	0.56	0.39	0.36	0.41		
ZuCO FPGD (Hollenstein et al., 2018)	0.80	0.84	0.88	0.79	0.73	0.78	0.86	0.76	0.72	0.70	0.85	0.84	0.80	0.84	0.76	0.72	0.67	0.61	0.65		
UCL SPR (Frank et al., 2013)	0.78	0.80	0.79	0.76	0.76	0.78	0.80	0.71	0.52	0.64	0.70	0.70	0.73	0.80	0.61	0.52	0.36	0.42	0.35		
UCL FPGD (Frank et al., 2013)	0.94	0.88	0.82	0.79	0.83	0.88	0.83	0.59	0.56	0.58	0.70	0.73	0.90	0.92	0.91	0.96	0.48	0.73	0.73		

Table 2: How likely Δ LL from internal layers outperformed the previous best Δ LL (achieved within the same model family, relying on their last layers). The results are focused on billion-scale models and behavioral data with somewhat drastic flips in LM-scaling effects for Δ LLs. “PT” denotes “Pythia.”

win rate is typically around 80%, indicating a significant proportion of internal layers achieved good Δ LL scores. These findings suggest that the cognitive plausibility of LLMs has been underestimated and that our argument (Figure 3) was not based on specific outlier layers but reflected a broader trend across many internal layers.

5.2 Layer depth and human measures

We observed systematic tendencies in the relationship between layer depth and human measurement methods. For instance, FPGD aligns better with earlier layers, whereas N400 aligns better with later layers, as summarized in Table 1. To statistically validate this relationship, we trained a linear regression model to explain Δ LL scores from our 15,833 experimental settings $s \in \{\text{dataset}\} \times \{\text{model}\} \times \{\text{layer}\}$, using the following formula:

$$\begin{aligned} \Delta\text{LL}(s) \sim & \text{stimuli}(s) + \text{model}(s) + \text{lens}(s) \\ & + \text{layer_depth}(s) + \text{measure}(s) \\ & + \text{layer_depth}(s) \times \text{measure}(s), \end{aligned} \quad (5)$$

where stimuli represents the source stimuli of the data (“Stimuli” column in Table 1), model encodes the model name, layer_depth is the depth of the layer where the Δ LL is obtained, measure encodes the human measurement method (“Measure” column in Table 1), and lens indicates whether the logit-lens or tuned-lens was used. The term $\text{layer_depth} \times \text{measure}$ captures the interaction between effective layer depth and human measures, which is of interest. Note that measure is a categorical variable, with FPGD serving as the dummy category.

The coefficients for $\text{layer_depth} \times \text{N400}$ and $\text{layer_depth} \times \text{MAZE}$ were significantly larger than zero ($p\text{-value} < 0.001$), while that for $\text{layer_depth} \times \text{SPR}$ does not significantly differ with $\text{layer_depth} \times \text{FPGD}$ (see full regression

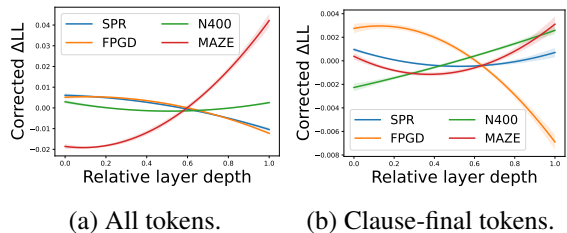


Figure 4: Relationship between Δ LL and relative layer depth (lower is shallower) for each human measure. Different measures are associated with different layers; for example, good Δ LLs for FPGD are achieved in earlier layers, while those for MAZE are in the latter layers.

results in Table 5 in the Appendix). This confirms that SPR and FPGD align with shallower layers than those yielding a good fit with N400 and MAZE. We also visualize the relationships between Δ LL and relative layer depth for each human measure in Figure 4a (polynomial fit using 2nd-order term). Here, we use corrected Δ LLs that are computed by subtracting variances explained by other factors than measure identified in Eq. 5. The lines also indicate the differences across different human measures, e.g., good Δ LL for MAZE is clearly associated with latter layers.

It is worth noting that we also conducted an exploratory analysis with other human measures (e.g., P600, second-pass gaze duration) on the UCL corpus (Table 4 in Appendix). For such an extended scope, we cannot confirm the implied relationship between fast–slow human responses and early–late LM layers, and this appears to hold primarily for well-established human measures of SPR, FPGD, N400, and MAZE.

5.3 Are results biased by targeted tokens?

A potential confound in § 5.2 stems from differences in targeted tokens for different human

Stimuli	Measure	Logit-lens (Δ LL)					Tuned-lens (Δ LL)				
		0-0.2	0.2-0.4	0.4-0.6	0.6-0.8	0.8-1.0	0-0.2	0.2-0.4	0.4-0.6	0.6-0.8	0.8-1.0
DC	FPGD (Kennedy et al., 2003)	1.49	1.71	1.76	1.63	1.20	1.59	1.60	1.65	1.58	1.30
NS	SPR (Futrell et al., 2021)	0.72	0.68	0.67	0.55	0.46	0.24	0.24	0.30	0.41	0.53
	MAZE (Boyce and Levy, 2023)	0.45	0.46	0.55	0.85	1.25	0.67	0.70	0.76	1.02	1.30
ZuCO	FPGD (Hollenstein et al., 2018)	34.84	35.39	31.97	23.08	9.75	30.48	27.16	22.56	17.29	8.77
	N400 (Hollenstein et al., 2018)	0.06	0.10	0.15	0.20	0.15	0.20	0.32	0.34	0.29	0.18
UCL	SPR (Frank et al., 2013)	3.40	2.73	2.13	1.06	0.23	0.52	0.20	0.10	0.11	0.15
	FPGD (Frank et al., 2013)	7.96	9.21	9.07	6.61	2.86	2.46	2.29	2.22	2.04	1.21
	N400 (Frank et al., 2015)	3.77	1.96	2.64	8.07	16.31	1.34	2.60	6.30	9.52	13.26
Fillers	SPR (Vasishth et al., 2010)	0.37	0.40	0.89	2.89	8.74	0.55	1.19	1.31	1.68	2.94
	FPGD (Vasishth et al., 2010)	0.26	0.22	0.21	0.62	1.50	0.37	0.32	0.27	0.71	1.19
	MAZE (Hahn et al., 2022)	4.78	3.46	2.05	5.77	12.19	0.49	0.94	3.43	5.33	6.13

Table 3: Results for the same settings as Table 1, except that only sentence/clause-final tokens are targeted. Some N400 data are omitted because they initially targeted only sentence/clause-final tokens. Δ LLs are multiplied by 1000 for brevity.

measures. For instance, N400 data are typically recorded only at sentence-final tokens to preprocess continuous, time-series EEG data, potentially introducing biases specific to sentence-final tokens, such as wrap-up effects (Just and Carpenter, 1980; Rayner et al., 2000; Meister et al., 2022). In contrast, behavioral measures are recorded across tokens within a sentence. To address this potential confound, we conducted additional experiments targeting sentence/clause-final tokens for all measures, even for SPR, FPGD, and MAZE. Sentence/clause-final tokens are identified using a constituency parser (Kitaev et al., 2019; Kitaev and Klein, 2018) and punctuations (e.g., “:”, “;”), following Meister et al. (2022).

Table 3 presents the results. Even when analyses were restricted to sentence-final tokens, earlier layers continued to align better with SPR and FPGD data. Regression analysis (same as § 5.2) confirmed that the coefficients for $\text{layer_depth} \times \text{N400}$ and $\text{layer_depth} \times \text{MAZE}$ remained significantly larger than those for $\text{layer_depth} \times \text{FPGD}$. The coefficient for $\text{layer_depth} \times \text{SPR}$ was also larger than that for $\text{layer_depth} \times \text{FPGD}$ (see full regression results in Table 6 in the Appendix). These patterns are visualized in Figure 4b.

5.4 Cross-lingual experiments

We also examined the generality of our findings across languages by following the experiments of de Varda and Marelli (2023), using FPGD data in 13 languages, recorded in MECO (Siegelman et al., 2022) and five variants of multilingual XGLMs (Lin et al., 2022). See detailed settings

and results in Appendix A (Table 7 and Figure 7).

In summary, the best layer was typically not exactly the last layer (85%=55/66 of the settings), aligned with our main results. However, compared to our main results in Table 1, the best layers leaned toward later depths. In addition, LM-scaling effects are still negative in several languages. These mixed results might be biased by the report that multilingual LMs process languages within the English subspace in middle layers (Wendler et al., 2024), leading to reduced alignment with target languages. Future work will explore scaling experiments with monolingual LMs, as suitable models to test scaling effects across languages are currently unavailable.

6 When are earlier layers advantageous?

We lastly explore when and why earlier layers’ surprisal aligns better with human reading data.

6.1 Residual error analysis

Following Oh and Schuler (2023b), we analyze by-token squared residual errors from regression models predicting human data (§ 3.3). We specifically use the largest data of DC (FPGD) and identify tokens where the use of the best internal layer, rather than the last layer, notably reduces errors.¹⁰ To address this question, we fit a linear regression model to predict the decreases in squared residual errors observed in each data point w_t with an LM

¹⁰Oh and Schuler (2023b) reported a misalignment between MSEs (residual errors) and log-likelihood scores due to the Euclidean norm penalty adopted in the `lme4` package. This did not arise in our analysis with `statsmodels`.

θ , with by-token linguistic properties as features:

$$\text{error_decrease}(w_t, \theta) \sim \text{model}(\theta) + \text{length}(w_t) + \text{freq}(w_t) + \text{position}(w_t) + \text{POS}(w_t) . \quad (6)$$

Results show that decreases in modeling error are associated with less frequent, longer words (see Table 8 in Appendix for full regression results). This aligns with prior observations (Oh et al., 2024) that LLMs tend to predict infrequent tokens with overly confident surprisals, and surprisal from internal layers mitigates this issue.

6.2 Contextualization in internal layers

We propose an additional perspective linking our findings to the context sensitivity of humans and LMs during sentence processing. Earlier layers may better model human reading behavior because they are less contextualized, reflecting the human-like tendency to process sentences under working memory constraints.

Working memory limitations in humans Human sentence processing is constrained by limited cognitive resources, relying on selective and efficient use of context (Lewis and Vasishth, 2005; Lieder and Griffiths, 2019; Futrell et al., 2020; Hahn et al., 2022). Recent studies indicate that the MAZE task imposes greater working memory demands, requiring more extensive context use than SPR or FPGD (Hahn et al., 2022; McCurdy and Hahn, 2024). This aligns with our observation that MAZE processing times are better modeled by later, more context-sensitive layers (see the next paragraph), whereas SPR and FPGD align with earlier, less contextualized layers.

Working memory limitations in LMs Modern neural LMs are not optimized to conserve cognitive resources and often rely excessively on context information, resulting in superhuman predictions (Kuribayashi et al., 2022; Oh et al., 2024). However, internal layers may exhibit a human-like moderation of context use. The NLP community has observed that LMs gradually enhance contextualization across layers, from shallow representations in early layers to deeply contextualized representations in later layers (Brunner et al. 2019; Ethayarajh 2019; Toneva and Wehbe 2019).

We also confirmed the by-layer context-sensitivity of surprisal by analyzing the correlation between (i) intermediate layers’ surprisal and

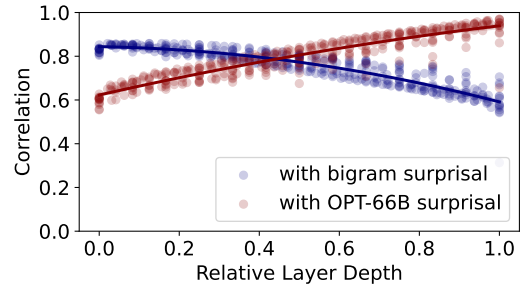


Figure 5: The markers correspond to all the internal layers of our targeted LMs, which are sorted by relative layer depth (x-axis). Two types of scores (y-axis) are plotted: (i) Pearson correlation coefficient between each layer’s surprisal vs. less-contextualized bigram surprisal (blue), and (ii) each layer’s surprisal vs. well-contextualized LLM surprisal (red). We used tuned-lens results.

less-contextualized bigram surprisal¹¹ and (ii) intermediate layers’ surprisal and more contextualized surprisal from the LLM with the lowest PPL (OPT-66B). Figure 5 shows the above two types of correlations for each model’s layer with the x-axis as the relative layer depth. This shows that earlier layers correlate more strongly with bigram surprisal (Pearson correlation coefficient r for this relationship is -0.92), while later layers align with more accurate, well-contextualized surprisal ($r=0.95$). These findings reinforce the idea that earlier layers exhibit limited context sensitivity, while later layers are more contextualized and better suited for modeling data like MAZE, which demands higher contextualization.

7 Conclusions

Recent cognitive modeling studies have demonstrated the worse fit of surprisal from larger LMs to human reading time. In this paper, we argue that these negative results stem from the exclusive focus on the *final layers* of LMs. Instead, we observe that those from *internal layers* comparably or even better fit with human behavior and neurophysiology data, suggesting that the cognitive plausibility of larger LMs has been underestimated. Furthermore, different human measurements align with different layers, implying an intriguing parallel between temporal dynamics in human sentence processing and LM internal layers.

¹¹Bigram LM is trained on OpenWebText (Gokaslan and Cohen, 2019) with KenLM toolkit (Heafield, 2011)

Limitations

The experiments can be extended to more types of human measures, such as first fixation time, go-past reading time, eye regressions, total fixation time, EEG data other than the N400 potential (Federmeier et al., 2007) as well as fMRI data (Shain et al., 2022). As a first step, we have begun with the measures of SPR, FPGD, N400, and MAZE, as they are typically used in cognitive modeling.

Recent studies have raised several issues, orthogonal to our study, on LM-based cognitive modeling, for example, on tokenizations (Nair and Resnik, 2023; Giulianelli et al., 2024a; Oh and Schuler, 2024), LM training scenario (Oh and Schuler, 2023a), as well as more refined indicators of word predictability (Pimentel et al., 2023; Giulianelli et al., 2024b; Opedal et al., 2024; Meister et al., 2024). More critically, the reliance solely on surprisal obtained from (not necessarily cognitively motivated) LMs will not tell the whole story of human sentence processing (van Schijndel and Linzen, 2021; Huang et al., 2024; Prasad and Linzen, 2024; Wang et al., 2024). We believe that the combination of such more linguistically motivated perspectives and our analysis will enrich the findings (e.g., we can also obtain probabilities from internal layers of neural parsers). This study itself contributes to clarifying to what extent surprisal from modern LMs, which are seemingly behaving similarly to humans (Hu et al., 2024), can explain online human sentence processing. More specifically, this study also opens up several new questions. For example, how can the best layer for cognitive modeling be automatically found from a number of LLM layers? What are the information-theoretical insights for cognitive modeling and surprisal theory?

References

- C Aurnhammer and S L Frank. 2019. [Comparing gated and simple recurrent neural network architectures as models of human sentence processing](#). In *Proceedings of CogSci*, pages 112–118.
- Khai Loong Aw, Syrielle Montariol, Badr AlKhamissi, Martin Schrimpf, and Antoine Bosselut. 2024. [Instruction-tuning aligns LLMs to the human brain](#). In *COLM 2024*.
- Andrea Banino, Jan Balaguer, and Charles Blundell. 2021. [PonderNet: Learning to ponder](#). In *8th ICML Workshop on Automated Machine Learning (AutoML)*.
- Lisa Beinborn and Nora Hollenstein. 2024. *Cognitive plausibility in natural language processing*. Synthesis lectures on human language technologies. Springer International Publishing, Cham.
- Nora Belrose, Zach Furman, Logan Smith, Danny Halawi, Lev McKinney, Igor Ostrovsky, Stella Biderman, and Jacob Steinhardt. 2023. [Eliciting latent predictions from transformers with the tuned lens](#). *arXiv preprint*.
- Stella Biderman, Hailey Schoelkopf, Quentin Gregory Anthony, Herbie Bradley, Kyle O’Brien, Eric Hallahan, Mohammad Aflah Khan, Shivanshu Purohit, USVSN Sai Prashanth, Edward Raff, et al. 2023. [Pythia: A suite for analyzing large language models across training and scaling](#). In *ICML 2023*, pages 2397–2430. PMLR.
- Veronica Boyce and Roger Philip Levy. 2023. [A maze of natural stories: Comprehension and surprisal in the maze task](#). *Glossa Psycholinguistics*.
- Gino Brunner, Yang Liu, Damian Pascual, Oliver Richter, Massimiliano Ciaramita, and Roger Wattenhofer. 2019. [On identifiability in transformers](#). In *ICLR 2019*.
- Manuel G Calvo and Enrique Meseguer. 2002. [Eye movements and processing stages in reading: Relative contribution of visual, lexical, and contextual factors](#). *The Spanish Journal of Psychology*, 5(1):66–77.
- Charlotte Caucheteux, Alexandre Gramfort, and Jean-Rémi King. 2023. [Evidence of a predictive coding hierarchy in the human brain listening to speech](#). *Nature human behaviour*, 7(3):430–441.
- Matthew W Crocker. 2007. [Computational psycholinguistics](#). *The Handbook of Computational Linguistics and Natural Language Processing*.
- Guy Dar, Mor Geva, Ankit Gupta, and Jonathan Berant. 2023. [Analyzing transformers in embedding space](#). In *Proceedings of ACL 2023*, pages 16124–16170.

- Olaf Dimigen, Werner Sommer, Annette Hohlfeld, Arthur M Jacobs, and Reinhold Kliegl. 2011. Coregistration of eye movements and eeg in natural reading: analyses and review. *Journal of experimental psychology: General*, 140(4):552.
- Kawin Ethayarajh. 2019. How contextual are contextualized word representations? comparing the geometry of BERT, ELMo, and GPT-2 embeddings. In *Proceedings of EMNLP-IJCNLP 2019*, pages 55–65.
- Kara D Federmeier, Edward W Wlotko, Esmeralda De Ochoa-Dewald, and Marta Kutas. 2007. Multiple effects of sentential constraint on word processing. *Brain Research*, 1146:75–84.
- Kenneth I Forster, Christine Guerrero, and Lisa Elliot. 2009. The maze task: measuring forced incremental sentence processing time. *Behavior research methods*, 41(1):163–171.
- Stefan L Frank and Rens Bod. 2011. Insensitivity of the human sentence-processing system to hierarchical structure. *Psychological Science*, 22(6):829–834.
- Stefan L Frank, Irene Fernandez Monsalve, Robin L Thompson, and Gabriella Vigliocco. 2013. Reading time data for evaluating broad-coverage models of english sentence processing. *Behavior research methods*, 45:1182–1190.
- Stefan L. Frank, Leun J. Otten, Giulia Galli, and Gabriella Vigliocco. 2015. The erp response to the amount of information conveyed by words in sentences. *Brain and Language*, 140:1–11.
- Richard Futrell, Edward Gibson, and Roger P. Levy. 2020. Lossy-Context Surprisal: An Information-Theoretic Model of Memory Effects in Sentence Processing. *Journal of Cognitive Science*.
- Richard Futrell, Edward Gibson, Harry J Tily, Idan Blank, Anastasia Vishnevetsky, Steven T Piantadosi, and Evelina Fedorenko. 2021. The natural stories corpus: a reading-time corpus of english texts containing rare syntactic constructions. *Language Resource and Evaluation*, 55(1):63–77.
- Mario Giulianelli, Luca Malagutti, Juan Luis Gastaldi, Brian DuSell, Tim Vieira, and Ryan Cotterell. 2024a. On the proper treatment of tokenization in psycholinguistics. In *Proceedings of EMNLP 2024*, pages 18556–18572.
- Mario Giulianelli, Andreas Opedal, and Ryan Cotterell. 2024b. Generalized measures of anticipation and responsivity in online language processing. In *Findings of EMNLP 2024*, pages 11648–11669.
- Aaron Gokaslan and Vanya Cohen. 2019. Open-webtext corpus. <http://Skylion007.github.io/OpenWebTextCorpus>.
- Adam Goodkind and Klinton Bicknell. 2018. Predictive power of word surprisal for reading times is a linear function of language model quality. In *Proceedings of CMCL*, pages 10–18.
- Alex Graves. 2016. Adaptive computation time for recurrent neural networks. *arXiv preprint*.
- Michael Hahn, Richard Futrell, Roger Levy, and Edward Gibson. 2022. A resource-rational model of human processing of recursive linguistic structure. *Proceedings of the National Academy of Sciences of the United States of America*, 119(43):e2122602119.
- John Hale. 2001. A probabilistic Earley parser as a psycholinguistic model. In *Proceedings of NAACL 2001*, pages 159–166.
- John Hale, Chris Dyer, Adhiguna Kuncoro, and Jonathan R. Brennan. 2018. Finding Syntax in Human Encephalography with Beam Search. In *Proceedings of ACL 2018*, pages 2727–2736.
- Kenneth Heafield. 2011. KenLM: Faster and smaller language model queries. In *Proceedings of the sixth workshop on statistical machine translation*, pages 187–197.
- Nora Hollenstein, Jonathan Rotsztein, Marius Troendle, Andreas Pedroni, Ce Zhang, and Nicolas Langer. 2018. ZuCo, a simultaneous EEG and eye-tracking resource for natural sentence reading. *Scientific Data*, 5:180291.
- Eghbal A Hosseini, Martin Schrimpf, Yian Zhang, Samuel Bowman, Noga Zaslavsky, and Evelina Fedorenko. 2024. Artificial neural network language models predict human brain responses to language even after a developmentally realistic amount of training. *Neurobiology of Language*, 5(1):43–63.

- Jennifer Hu, Kyle Mahowald, Gary Lupyán, Anna Ivanova, and Roger Levy. 2024. [Language models align with human judgments on key grammatical constructions](#). *Proceedings of the National Academy of Sciences*, 121(36):e2400917121.
- Kuan-Jung Huang, Suhas Arehalli, Mari Kugemoto, Christian Muxica, Grusha Prasad, Brian Dillon, and Tal Linzen. 2024. [Large-scale benchmark yields no evidence that language model surprisal explains syntactic disambiguation difficulty](#). *Journal of Memory and Language*, 137:104510.
- Ryan J Hubbard, Joost Rommers, Cassandra L Jacobs, and Kara D Federmeier. 2019. [Downstream behavioral and electrophysiological consequences of word prediction on recognition memory](#). *Frontiers in human neuroscience*, 13:291.
- Marcel A. Just and Patricia A. Carpenter. 1980. [A theory of reading: From eye fixations to comprehension](#). *Journal of Psychological Review*.
- Yiğitcan Kaya, Sanghyun Hong, and Tudor Dumitras. 2019. [Shallow-Deep Networks: Understanding and mitigating network overthinking](#). In *Proceedings of ICML 2019*.
- Alan Kennedy, Robin Hill, and Joël Pynte. 2003. [The dundee corpus](#). In *Proceedings of the 12th European conference on eye movement*.
- Nikita Kitaev, Steven Cao, and Dan Klein. 2019. [Multilingual constituency parsing with self-attention and pre-training](#). In *Proceedings of ACL 2019*, pages 3499–3505.
- Nikita Kitaev and Dan Klein. 2018. [Constituency parsing with a self-attentive encoder](#). In *Proceedings of ACL 2018*, pages 2676–2686.
- Tatsuki Kuribayashi, Yohei Oseki, and Timothy Baldwin. 2024. [Psychometric predictive power of large language models](#). In *Findings of NAACL 2024*, pages 1983–2005.
- Tatsuki Kuribayashi, Yohei Oseki, Ana Brassard, and Kentaro Inui. 2022. [Context limitations make neural language models more human-like](#). In *Proceedings of EMNLP 2022*, pages 10421–10436.
- Tatsuki Kuribayashi, Yohei Oseki, Takumi Ito, Ryo Yoshida, Masayuki Asahara, and Kentaro Inui. 2021. [Lower perplexity is not always human-like](#). In *Proceedings of ACL-IJCNLP 2021*, pages 5203–5217.
- Marta Kutas and Kara D Federmeier. 2011. [Thirty years and counting: finding meaning in the N400 component of the event-related brain potential \(ERP\)](#). *Annual review of psychology*, 62(1):621–647.
- Ellen F Lau, Colin Phillips, and David Poeppel. 2008. [A cortical network for semantics: \(de\)constructing the N400](#). *Nature Reviews Neuroscience*, 9(12):920–933.
- Roger Levy. 2008. [Expectation-based syntactic comprehension](#). *Journal of Cognition*, 106(3):1126–1177.
- Richard L Lewis and Shravan Vasishth. 2005. [An activation-based model of sentence processing as skilled memory retrieval](#). *Cogn. Sci.*, 29(3):375–419.
- Falk Lieder and Thomas L Griffiths. 2019. [Resource-rational analysis: Understanding human cognition as the optimal use of limited computational resources](#). *Behavioral and Brain Sciences*, 43(e1):e1.
- Xi Victoria Lin, Todor Mihaylov, Mikel Artetxe, Tianlu Wang, Shuohui Chen, Daniel Simig, Myle Ott, Naman Goyal, Shrutí Bhosale, Jingfei Du, Ramakanth Pasunuru, Sam Shleifer, Punit Singh Koura, Vishrav Chaudhary, Brian O’Horo, Jeff Wang, Luke Zettlemoyer, Zornitsa Kozareva, Mona Diab, Veselin Stoyanov, and Xian Li. 2022. [Few-shot learning with multilingual generative language models](#). In *Proceedings of EMNLP 2022*, pages 9019–9052.
- David Marr. 1982. *Vision: A Computational Investigation into the Human Representation and Processing of Visual Information*. Henry Holt and Co., Inc., USA.
- Kate McCurdy and Michael Hahn. 2024. [Lossy context surprisal predicts task-dependent patterns in relative clause processing](#). In *Proceedings of CoNLL 2024*, pages 36–45.
- Clara Meister, Mario Giulianelli, and Tiago Pimentel. 2024. [Towards a similarity-adjusted](#)

- surprisal theory. In *Proceedings of EMNLP 2024*, pages 16485–16498.
- Clara Meister, Tiago Pimentel, Thomas Clark, Ryan Cotterell, and Roger Levy. 2022. Analyzing wrap-up effects through an information-theoretic lens. In *Proceedings of ACL 2022*, pages 20–28.
- Danny Merckx and Stefan L. Frank. 2021. Human sentence processing: Recurrence or attention? In *Proceedings of CMCL*, pages 12–22.
- James Michaelov, Catherine Arnett, and Ben Bergen. 2024a. Revenge of the fallen? recurrent models match transformers at predicting human language comprehension metrics. In *COLM 2024*.
- James A. Michaelov, Megan D. Bardolph, Cyma K. Van Petten, Benjamin K. Bergen, and Seana Coulson. 2024b. Strong Prediction: Language Model Surprisal Explains Multiple N400 Effects. *Neurobiology of Language*, 5(1):107–135.
- Sathvik Nair and Philip Resnik. 2023. Words, subwords, and morphemes: What really matters in the surprisal-reading time relationship? In *Findings of EMNLP2023*.
- nostalgebraist. 2020. interpreting gpt: the logit lens.
- Samer Nour Eddine, Trevor Brothers, Lin Wang, Michael Spratling, and Gina R Kuperberg. 2024. A predictive coding model of the N400. *Cognition*, 246(105755):105755.
- Byung-Doh Oh, Christian Clark, and William Schuler. 2021. Surprisal estimators for human reading times need character models. In *Proceedings of ACL-IJCNLP 2021*, pages 3746–3757.
- Byung-Doh Oh, Christian Clark, and William Schuler. 2022. Comparison of structural parsers and neural language models as surprisal estimators. *Frontiers in Artificial Intelligence*, 5:777963.
- Byung-Doh Oh and William Schuler. 2023a. Transformer-based language model surprisal predicts human reading times best with about two billion training tokens. In *Findings of EMNLP 2023*, pages 1915–1921.
- Byung-Doh Oh and William Schuler. 2023b. Why does surprisal from larger transformer-based language models provide a poorer fit to human reading times? *TACL*, 11:336–350.
- Byung-Doh Oh and William Schuler. 2024. Leading whitespaces of language models’ subword vocabulary pose a confound for calculating word probabilities. In *Proceedings of EMNLP 2024*, pages 3464–3472.
- Byung-Doh Oh, Shisen Yue, and William Schuler. 2024. Frequency explains the inverse correlation of large language models’ size, training data amount, and surprisal’s fit to reading times. In *Proceedings of EACL 2024*, pages 2644–2663.
- Andreas Opedal, Eleanor Chodroff, Ryan Cotterell, and Ethan Wilcox. 2024. On the role of context in reading time prediction. In *Proceedings of EMNLP 2024*, pages 3042–3058.
- Tiago Pimentel, Clara Meister, Ethan G Wilcox, Roger P Levy, and Ryan Cotterell. 2023. On the effect of anticipation on reading times. *TACL*, 11:1624–1642.
- Grusha Prasad and Tal Linzen. 2024. SPAWN-ing structural priming predictions from a cognitively motivated parser. In *Proceedings of CoNLL 2024*, pages 178–197.
- Alec Radford, Jeffrey Wu, Rewon Child, David Luan, Dario Amodei, Ilya Sutskever, et al. 2019. Language models are unsupervised multitask learners. OpenAI blog.
- Keith Rayner. 1998. Eye movements in reading and information processing: 20 years of research. *Psychological bulletin*, 124(3):372–422.
- Keith Rayner and Charles Clifton, Jr. 2009. Language processing in reading and speech perception is fast and incremental: implications for event-related potential research. *Biological Psychology*, 80(1):4–9.
- Keith Rayner, Gretchen Kambe, and Susan A. Duffy. 2000. The Effect of Clause Wrap-Up on Eye Movements during Reading. *Quarterly Journal of Experimental Psychology Section A: Human Experimental Psychology*, 53(4):1061–1080.

- Marten van Schijndel and Tal Linzen. 2021. [Single-Stage prediction models do not explain the magnitude of syntactic disambiguation difficulty](#). *Cognitive Science*, 45(6):e12988.
- Martin Schrimpf, Idan Asher Blank, Greta Tuckute, Carina Kauf, Eghbal A Hosseini, Nancy Kanwisher, Joshua B Tenenbaum, and Evelina Fedorenko. 2021. [The neural architecture of language: Integrative modeling converges on predictive processing](#). *Proceedings of the National Academy of Sciences*, 118(45):e2105646118.
- Skipper Seabold and Josef Perktold. 2010. [statsmodels: Econometric and statistical modeling with Python](#). In *9th Python in Science Conference*.
- Cory Shain, Idan A Blank, Evelina Fedorenko, Edward Gibson, and William Schuler. 2022. [Robust effects of working memory demand during naturalistic language comprehension in language-selective cortex](#). *Journal of Neuroscience*, 42(39):7412–7430.
- Cory Shain, Clara Meister, Tiago Pimentel, Ryan Cotterell, and Roger Levy. 2024. [Large-scale evidence for logarithmic effects of word predictability on reading time](#). *Proceedings of the National Academy of Sciences*, 121(10):e2307876121.
- Noam Siegelman, Sascha Schroeder, Cengiz Acartürk, Hee-Don Ahn, Svetlana Alexeeva, Simona Amenta, Raymond Bertram, Rolando Bonandrini, Marc Brysbaert, Daria Chernova, et al. 2022. [Expanding horizons of cross-linguistic research on reading: The multilingual eye-movement corpus \(meco\)](#). *Behavior research methods*, 54(6):2843–2863.
- Nathaniel J Smith and Roger Levy. 2013. [The effect of word predictability on reading time is logarithmic](#). *Cognition*, 128(3):302–319.
- Robyn Speer. 2022. [rspeer/wordfreq: v3.0](#).
- Jakub M Szewczyk and Kara D Federmeier. 2022. [Context-based facilitation of semantic access follows both logarithmic and linear functions of stimulus probability](#). *Journal of Memory and Language*, 123(104311):104311.
- Jakub M Szewczyk, Emily N Mech, and Kara D Federmeier. 2022. [The power of “good”: Can adjectives rapidly decrease as well as increase the availability of the upcoming noun?](#) *Journal of Experimental Psychology: Learning, Memory, and Cognition*, 48(6):856–875.
- Ian Tenney, Dipanjan Das, and Ellie Pavlick. 2019. [BERT rediscovers the classical NLP pipeline](#). In *Proceedings of ACL 2019*, pages 4593–4601.
- Mariya Toneva and Leila Wehbe. 2019. [Interpreting and improving natural-language processing \(in machines\) with natural language-processing \(in the brain\)](#). *NeurIPS 2019*, pages 14928–14938.
- Pranali Vani, Ethan Gotlieb Wilcox, and Roger Levy. 2021. [Using the interpolated maze task to assess incremental processing in english relative clauses](#). *Proceedings of the Annual Meeting of the Cognitive Science Society*, 43(43).
- Andrea de Varda and Marco Marelli. 2023. [Scaling in cognitive modelling: a multilingual approach to human reading times](#). In *Proceedings of ACL 2023*, pages 139–149.
- Andrea Gregor de Varda, Marco Marelli, and Simona Amenta. 2024. [Cloze probability, predictability ratings, and computational estimates for 205 english sentences, aligned with existing EEG and reading time data](#). *Behavior Research Methods*, 56(5):5190–5213.
- Shravan Vasishth, Katja Suckow, Richard L Lewis, and Sabine Kern. 2010. [Short-term forgetting in sentence comprehension: Crosslinguistic evidence from verb-final structures](#). *Language and Cognitive Processes*, 25(4):533–567.
- Andreas Waldis, Yotam Perlitz, Leshem Choshen, Yufang Hou, and Iryna Gurevych. 2024. [Holmes a benchmark to assess the linguistic competence of language models](#). *TACL*, 12:1616–1647.
- Daphne Wang, Mehrnoosh Sadrzadeh, Miloš Stanojević, Wing-Yee Chow, and Richard Breheny. 2024. [How can large language models become more human?](#) In *Proceedings of CMCL 2024*, pages 166–176.

- Chris Wendler, Veniamin Veselovsky, Giovanni Monea, and Robert West. 2024. [Do llamas work in english? on the latent language of multilingual transformers](#). In *Proceedings of ACL 2024*, pages 15366–15394.
- Ethan Wilcox, Clara Meister, Ryan Cotterell, and Tiago Pimentel. 2023a. [Language model quality correlates with psychometric predictive power in multiple languages](#). In *Proceedings of EMNLP 2023*, pages 7503–7511.
- Ethan Wilcox, Clara Meister, Ryan Cotterell, and Tiago Pimentel. 2023b. [Language model quality correlates with psychometric predictive power in multiple languages](#). In *Proceedings of EMNLP 2023*, pages 7503–7511.
- Ethan Gottlieb Wilcox, Jon Gauthier, Jennifer Hu, Peng Qian, and Roger Levy. 2020. [On the Predictive Power of Neural Language Models for Human Real-Time Comprehension Behavior](#). In *Proceedings of CogSci*, pages 1707–1713.
- Ethan Gottlieb Wilcox, Michael Hu, Aaron Mueller, Tal Linzen, Alex Warstadt, Leshem Choshen, Chengxu Zhuang, Ryan Cotterell, and Adina Williams. 2024. [Bigger is not always better: The importance of human-scale language modeling for psycholinguistics](#). *PsyArXiv*.
- Naoko Witzel, Jeffrey Witzel, and Kenneth Forster. 2012. [Comparisons of online reading paradigms: eye tracking, moving-window, and maze](#). *Journal of Psycholinguistic Research*, 41(2):105–128.
- Edward W Wlotko and Kara D Federmeier. 2012. [So that’s what you meant! event-related potentials reveal multiple aspects of context use during construction of message-level meaning](#). *Neuroimage*, 62(1):356–366.
- Ryo Yoshida, Hiroshi Noji, and Yohei Oseki. 2021. [Modeling human sentence processing with left-corner recurrent neural network grammars](#). In *Proceedings of EMNLP 2021*, pages 2964–2973.
- Susan Zhang, Stephen Roller, Naman Goyal, Mikel Artetxe, Moya Chen, Shuohui Chen, Christopher Dewan, Mona T. Diab, Xian Li, Xi Victoria Lin, Todor Mihaylov, Myle Ott, Sam Shleifer, Kurt Shuster, Daniel Simig, Punit Singh Koura, Anjali Sridhar, Tianlu Wang, and Luke Zettlemoyer. 2022. [OPT: Open Pre-trained Transformer Language Models](#). *arXiv preprint*, cs.CL/2205.01068v4.
- Wangchunshu Zhou, Canwen Xu, Tao Ge, Julian McAuley, Ke Xu, and Furu Wei. 2020. [BERT loses patience: Fast and robust inference with early exit](#). *NeurIPS 2020*, abs/2006.04152.

A Cross-lingual experiments

We target FPGD data from MECO in 13 languages (Siegelman et al., 2022) using five multi-lingual XGLMs (Lin et al., 2022) (564M, 1.7B, 2.9B, 4.5B, 7.5B). We analyze the Δ LL of surprisal from their internal layers. Due to the unavailability of tuned-lenses for XGLMs, only logit-lenses were used. Table 7 shows Δ LLs per-layer-range, and Figure 7 shows the relationship between parameter numbers and Δ LL.

Measure	Logit-lens (Δ LL)					Tuned-lens (Δ LL)				
	0-0.2	0.2-0.4	0.4-0.6	0.6-0.8	0.8-1	0-0.2	0.2-0.4	0.4-0.6	0.6-0.8	0.8-1
SPR	24.51	23.35	18.84	7.80	1.81	15.78	8.92	4.87	2.53	1.27
FPGD	22.62	26.24	25.12	15.55	5.02	16.28	14.48	11.87	9.47	5.57
SPGD	241.76	191.77	124.82	30.13	3.97	68.43	20.05	5.28	1.71	3.87
TOTAL	211.73	175.06	119.29	32.39	3.06	67.39	23.51	7.82	1.61	1.56
ELAN (125–175ms)	0.79	0.38	0.18	0.30	0.49	0.22	0.38	0.77	0.67	0.50
LAN (300–400ms)	70.32	48.69	25.78	5.05	6.14	19.94	2.74	1.72	5.02	8.76
N400 (300–500ms)	57.45	33.30	14.01	12.89	32.26	11.31	6.12	16.19	29.49	37.11
EPNP (400–600ms)	78.22	58.65	35.25	7.76	3.09	29.31	6.67	1.29	1.56	4.45
P600 (500–700ms)	69.52	50.43	29.25	6.37	7.39	17.70	3.30	1.80	5.83	11.36
PNP (600–700ms)	60.47	46.76	29.58	7.32	1.56	25.38	8.09	2.30	0.73	1.61

Table 4: Results for other human measures recorded on the UCL corpus. Δ LLs are multiplied by 1000.

Features	coef	std err	t	P>	t	[0.025	0.975]
Intercept	0.0204	0.001	28.757	0.000	0.019	0.022	
stimuli[T.Federmeier+, 2007]	0.0025	0.001	3.945	0.000	0.001	0.004	
stimuli[T.Fillers]	0.0011	0.000	2.281	0.023	0.000	0.002	
stimuli[T.Hubbard+, 2019]	-0.0109	0.001	-17.559	0.000	-0.012	-0.010	
stimuli[T.Michaelov+, 2024]	-0.0096	0.001	-15.458	0.000	-0.011	-0.008	
stimuli[T.NNS]	-0.0038	0.001	-6.927	0.000	-0.005	-0.003	
stimuli[T.S&F,2022]	-0.0105	0.001	-16.822	0.000	-0.012	-0.009	
stimuli[T.Szewczyk+, 2022]	-0.0057	0.001	-9.240	0.000	-0.007	-0.005	
stimuli[T.UCL]	0.0054	0.000	11.807	0.000	0.004	0.006	
stimuli[T.W&F,2012]	-0.0109	0.001	-17.593	0.000	-0.012	-0.010	
stimuli[T.ZuCO]	-0.0007	0.000	-1.450	0.147	-0.002	0.000	
model[T.gpt2-large]	0.0010	0.001	1.633	0.103	-0.000	0.002	
model[T.gpt2-medium]	-0.0004	0.001	-0.542	0.588	-0.002	0.001	
model[T.gpt2-xl]	0.0013	0.001	2.199	0.028	0.000	0.002	
model[T.opt-1.3b]	0.0017	0.001	2.544	0.011	0.000	0.003	
model[T.opt-125m]	0.0015	0.001	1.964	0.049	3.21e-06	0.003	
model[T.opt-13b]	0.0017	0.001	2.505	0.012	0.000	0.003	
model[T.opt-2.7b]	0.0019	0.001	2.735	0.006	0.001	0.003	
model[T.opt-30b]	0.0011	0.001	1.644	0.100	-0.000	0.002	
model[T.opt-6.7b]	0.0017	0.001	2.662	0.008	0.000	0.003	
model[T.opt-66b]	0.0019	0.001	2.981	0.003	0.001	0.003	
model[T.pythia-1.4b-deduped]	-1.555e-05	0.001	-0.024	0.981	-0.001	0.001	
model[T.pythia-12b-deduped]	0.0012	0.001	1.993	0.046	2.03e-05	0.002	
model[T.pythia-14m]	-0.0033	0.001	-2.714	0.007	-0.006	-0.001	
model[T.pythia-160m-deduped]	-0.0026	0.001	-3.468	0.001	-0.004	-0.001	
model[T.pythia-1b-deduped]	8.195e-06	0.001	0.010	0.992	-0.002	0.002	
model[T.pythia-1b-deduped-v0]	0.0012	0.002	0.737	0.461	-0.002	0.004	
model[T.pythia-2.8b-deduped]	0.0005	0.001	0.814	0.416	-0.001	0.002	
model[T.pythia-31m]	-0.0031	0.001	-2.567	0.010	-0.005	-0.001	
model[T.pythia-410m-deduped]	-0.0003	0.001	-0.486	0.627	-0.002	0.001	
model[T.pythia-6.9b-deduped]	0.0007	0.001	1.173	0.241	-0.000	0.002	
model[T.pythia-70m-deduped]	-0.0027	0.001	-3.060	0.002	-0.004	-0.001	
measure[T.MAZE]	-0.0261	0.001	-39.073	0.000	-0.027	-0.025	
measure[T.N400]	-0.0124	0.001	-24.251	0.000	-0.013	-0.011	
measure[T.SPR]	-0.0030	0.001	-5.303	0.000	-0.004	-0.002	
method[T.tuned-lens]	7.998e-05	0.000	0.389	0.697	-0.000	0.000	
normalized_layer	-0.0124	0.001	-20.423	0.000	-0.014	-0.011	
measure[T.MAZE]:normalized_layer	0.0782	0.001	74.603	0.000	0.076	0.080	
measure[T.N400]:normalized_layer	0.0170	0.001	22.907	0.000	0.016	0.018	
measure[T.SPR]:normalized_layer	0.0009	0.001	0.978	0.328	-0.001	0.003	

Table 5: Coefficients of the regression results in Figure 4a. The coefficients for the interaction terms listed in the last three lines are of interest.

Features	coef	std err	t	P>	t	[0.025	0.975]
Intercept	0.0054	0.000	20.302	0.000	0.005	0.006	
stimuli[T.Federmeier+, 2007]	0.0366	0.000	137.401	0.000	0.036	0.037	
stimuli[T.Fillers]	0.0007	0.000	3.936	0.000	0.000	0.001	
stimuli[T.Hubbard+, 2019]	0.0232	0.000	87.206	0.000	0.023	0.024	
stimuli[T.Michaelov+, 2024]	0.0245	0.000	92.110	0.000	0.024	0.025	
stimuli[T.NNS]	-0.0014	0.000	-6.827	0.000	-0.002	-0.001	
stimuli[T.S&F,2022]	0.0237	0.000	88.926	0.000	0.023	0.024	
stimuli[T.Szewczyk+, 2022]	0.0284	0.000	106.623	0.000	0.028	0.029	
stimuli[T.UCL]	0.0020	0.000	11.513	0.000	0.002	0.002	
stimuli[T.W&F,2012]	0.0232	0.000	87.126	0.000	0.023	0.024	
stimuli[T.ZuCO]	0.0232	0.000	123.112	0.000	0.023	0.024	
model[T.gpt2-large]	0.0004	0.000	1.702	0.089	-5.95e-05	0.001	
model[T.gpt2-medium]	-0.0002	0.000	-0.561	0.575	-0.001	0.000	
model[T.gpt2-xl]	0.0008	0.000	3.477	0.001	0.000	0.001	
model[T.opt-1.3b]	0.0008	0.000	3.115	0.002	0.000	0.001	
model[T.opt-125m]	0.0003	0.000	1.231	0.218	-0.000	0.001	
model[T.opt-13b]	0.0008	0.000	2.952	0.003	0.000	0.001	
model[T.opt-2.7b]	0.0009	0.000	3.425	0.001	0.000	0.001	
model[T.opt-30b]	0.0006	0.000	2.412	0.016	0.000	0.001	
model[T.opt-6.7b]	0.0005	0.000	2.184	0.029	5.24e-05	0.001	
model[T.opt-66b]	0.0009	0.000	3.748	0.000	0.000	0.001	
model[T.pythia-1.4b-deduped]	0.0004	0.000	1.449	0.147	-0.000	0.001	
model[T.pythia-12b-deduped]	0.0010	0.000	4.172	0.000	0.001	0.001	
model[T.pythia-14m]	-0.0016	0.000	-3.566	0.000	-0.003	-0.001	
model[T.pythia-160m-deduped]	-0.0003	0.000	-1.082	0.279	-0.001	0.000	
model[T.pythia-1b-deduped]	1.503e-05	0.000	0.047	0.962	-0.001	0.001	
model[T.pythia-1b-deduped-v0]	0.0008	0.001	1.385	0.166	-0.000	0.002	
model[T.pythia-2.8b-deduped]	0.0003	0.000	1.218	0.223	-0.000	0.001	
model[T.pythia-31m]	-0.0014	0.000	-2.983	0.003	-0.002	-0.000	
model[T.pythia-410m-deduped]	-8.252e-05	0.000	-0.337	0.736	-0.001	0.000	
model[T.pythia-6.9b-deduped]	0.0008	0.000	3.247	0.001	0.000	0.001	
model[T.pythia-70m-deduped]	-0.0008	0.000	-2.471	0.013	-0.001	-0.000	
measure[T.MAZE]	-0.0046	0.000	-18.669	0.000	-0.005	-0.004	
measure[T.N400]	-0.0318	0.000	-135.362	0.000	-0.032	-0.031	
measure[T.SPR]	-0.0053	0.000	-24.991	0.000	-0.006	-0.005	
method[T.tuned-lens]	-0.0009	7.74e-05	-11.156	0.000	-0.001	-0.001	
normalized_layer	-0.0079	0.000	-35.798	0.000	-0.008	-0.008	
measure[T.MAZE]:normalized_layer	0.0124	0.000	32.324	0.000	0.012	0.013	
measure[T.N400]:normalized_layer	0.0145	0.000	52.124	0.000	0.014	0.015	
measure[T.SPR]:normalized_layer	0.0094	0.000	27.774	0.000	0.009	0.010	

Table 6: Coefficients of the regression results in Figure 4b (only sentence/clause-final tokens are targeted).

Lang.	Logit-lens (Δ LL)				
	0-0.2	0.2-0.4	0.4-0.6	0.6-0.8	0.8-1
Du	5.62	5.58	7.66	11.60	20.77
Ee	2.16	2.34	2.74	3.37	3.26
En	4.51	12.49	21.43	23.53	20.04
Fi	7.61	8.72	10.44	15.59	16.25
Ge	18.20	22.83	28.66	34.41	30.57
Gr	15.05	19.75	21.20	21.61	18.19
He	2.12	1.95	1.25	1.96	1.98
It	16.55	18.85	24.19	29.50	32.42
Ko	3.09	4.02	4.74	5.73	5.96
No	22.80	21.56	23.43	25.29	27.27
Ru	0.51	0.47	0.37	0.28	0.33
Sp	13.58	16.29	18.68	20.00	16.83
Tr	2.99	3.91	6.03	10.97	15.44

Table 7: Results in MECO. Δ LLs are multiplied by 1000 for brevity.

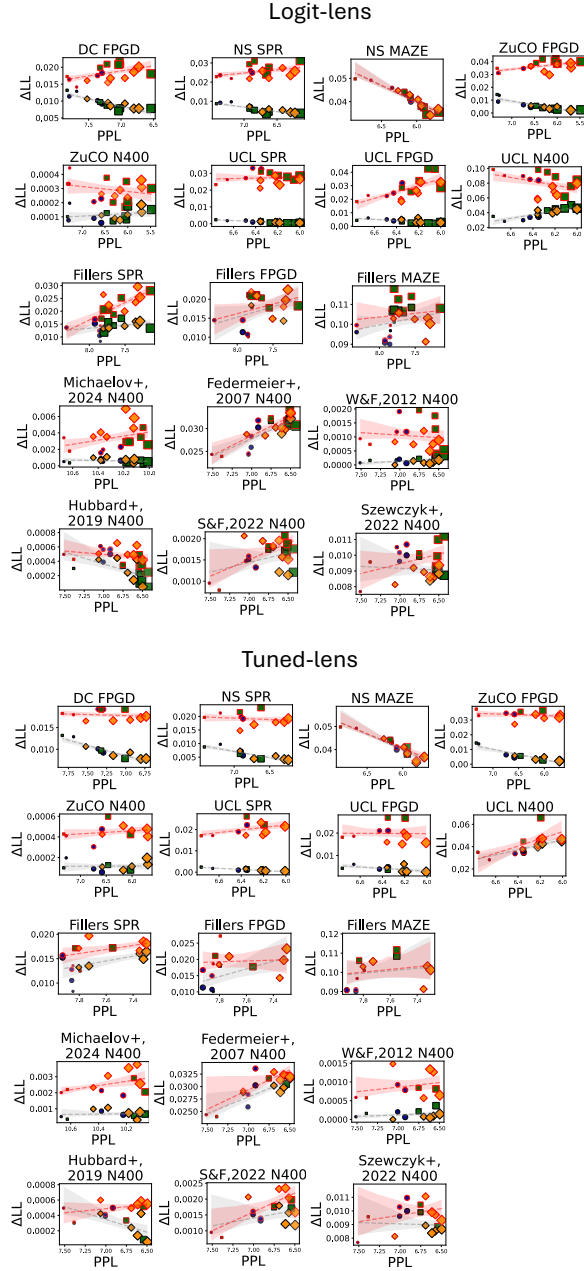


Figure 6: Scaling effect between ΔLL and PPL (measured on respective datasets with final layer), instead of model parameter counts, as adopted in Figure 3.

Features	coef	std err	t	P >	t [0.025 0.975]
Intercept	0.0801	0.430	0.186	0.852	-0.764 0.924
model[T.gpt2-large]	0.1510	0.061	2.490	0.013	0.032 0.270
model[T.gpt2-xl]	0.1293	0.061	2.132	0.033	0.010 0.248
model[T.opt-1.3b]	0.0182	0.061	0.301	0.764	-0.101 0.137
model[T.opt-125m]	0.1898	0.061	3.131	0.002	0.071 0.309
model[T.opt-6.7b]	0.0754	0.061	1.243	0.214	-0.043 0.194
model[T.pythia-1.4b-deduped]	0.1649	0.061	2.719	0.007	0.046 0.284
model[T.pythia-12b-deduped]	0.1237	0.061	2.040	0.041	0.005 0.243
model[T.pythia-160m-deduped]	0.0695	0.061	1.146	0.252	-0.049 0.188
model[T.pythia-1b-deduped-v0]	0.1212	0.061	1.998	0.046	0.002 0.240
model[T.pythia-2.8b-deduped]	0.0607	0.061	1.001	0.317	-0.058 0.180
model[T.pythia-410m-deduped]	0.1534	0.061	2.529	0.011	0.035 0.272
model[T.pythia-6.9b-deduped]	-0.0478	0.061	-0.788	0.431	-0.167 0.071
model[T.pythia-70m-deduped]	-0.0478	0.061	-0.788	0.431	-0.167 0.071
pos[T.\$]	-0.1911	0.776	-0.246	0.805	-1.711 1.329
pos[T.,]	-4.1266	0.985	-4.188	0.000	-6.058 -2.195
pos[T.]	-2.5070	1.327	-1.890	0.059	-5.107 0.093
pos[T.CC]	-0.7410	0.431	-1.719	0.086	-1.586 0.104
pos[T.CD]	-1.6381	0.443	-3.699	0.000	-2.506 -0.770
pos[T.DT]	-0.9570	0.428	-2.238	0.025	-1.795 -0.119
pos[T.EX]	-1.5530	0.489	-3.176	0.001	-2.511 -0.595
pos[T.FW]	4.2889	0.580	7.395	0.000	3.152 5.426
pos[T.IN]	-1.1206	0.427	-2.625	0.009	-1.957 -0.284
pos[T.IJ]	-1.4790	0.427	-3.461	0.001	-2.317 -0.641
pos[T.JJR]	-1.6572	0.463	-3.580	0.000	-2.565 -0.750
pos[T.JJS]	-2.1918	0.488	-4.489	0.000	-3.149 -1.235
pos[T.MD]	-1.6324	0.435	-3.749	0.000	-2.486 -0.779
pos[T.NN]	-2.0801	0.427	-4.876	0.000	-2.916 -1.244
pos[T.NNP]	-1.0809	0.428	-2.523	0.012	-1.921 -0.241
pos[T.NNPS]	-5.2269	0.484	-10.804	0.000	-6.175 -4.279
pos[T.NNS]	-2.1715	0.428	-5.071	0.000	-3.011 -1.332
pos[T.PDT]	-2.2381	0.535	-4.183	0.000	-3.287 -1.189
pos[T.POS]	-2.0896	0.449	-4.651	0.000	-2.970 -1.209
pos[T.PRP]	-1.0883	0.430	-2.529	0.011	-1.932 -0.245
pos[T.PRPS]	-1.4344	0.435	-3.296	0.001	-2.287 -0.581
pos[T.RB]	-1.7242	0.428	-4.026	0.000	-2.564 -0.885
pos[T.RBR]	-1.8143	0.482	-3.761	0.000	-2.760 -0.869
pos[T.RBS]	-3.0363	0.529	-5.743	0.000	-4.073 -2.000
pos[T.RP]	-1.4753	0.456	-3.235	0.001	-2.369 -0.582
pos[T.SYM]	2.6044	0.901	2.889	0.004	0.838 4.371
pos[T.TO]	-0.6908	0.431	-1.602	0.109	-1.536 0.155
pos[T.UH]	-7.8480	0.759	-10.338	0.000	-9.336 -6.360
pos[T.VB]	-1.2679	0.429	-2.955	0.003	-2.109 -0.427
pos[T.VBD]	-1.6735	0.431	-3.885	0.000	-2.518 -0.829
pos[T.VBG]	-2.0877	0.433	-4.818	0.000	-2.937 -1.238
pos[T.VBN]	-1.7750	0.431	-4.118	0.000	-2.620 -0.930
pos[T.VBP]	-1.1485	0.432	-2.659	0.008	-1.995 -0.302
pos[T.VBZ]	-1.2311	0.431	-2.860	0.004	-2.075 -0.387
pos[T.WDT]	-1.2174	0.449	-2.714	0.007	-2.097 -0.338
pos[T.WP]	-1.0289	0.455	-2.264	0.024	-1.920 -0.138
pos[T.WP\$]	0.1774	0.869	0.204	0.838	-1.525 1.880
pos[T.WRB]	-0.8454	0.456	-1.853	0.064	-1.740 0.049
has_punct[T.True]	-1.6396	0.038	-43.221	0.000	-1.714 -1.565
has_num[T.True]	2.3217	0.171	13.602	0.000	1.987 2.656
freq	0.0142	0.007	1.930	0.054	-0.000 0.029
length	0.3629	0.007	51.621	0.000	0.349 0.377
token_position_in_sentence	-0.0042	0.001	-3.958	0.000	-0.006 -0.002

Table 8: The results of regression model to predict the per-token squared residual errors. Note that word frequency and length are confounded (Pearson’s $r = -0.7$), and once the length factor is excluded, the coefficient for the word frequency feature becomes significantly negative and has a high t-score. That is, a large decrease in regression error is generally associated with infrequent, long words.

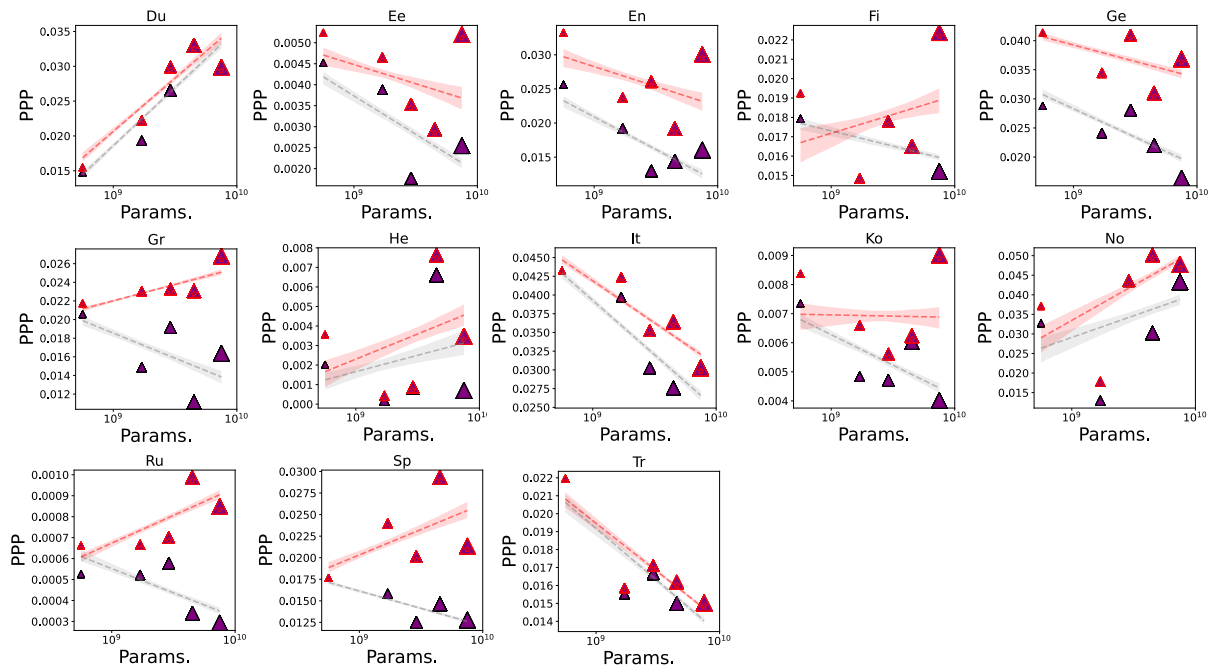


Figure 7: Scaling effect between Δ LL and parameter counts in MECO. The grey lines are results replying on the last layer's Δ LLs and, the red lines rely on the best internal layers' Δ LLs. In four languages (Fi, Gr, Ru, Sp) out of the targeted 13 languages, the scaling effect flipped from negative to positive, and we never observed the case of flipping from positive to negative.